SUBSTRUCTURE ONLINE TEST USING PARALLEL HYSTERESIS MODELING BY NEURAL NETWORK

Y. Nakano[1] and W. J. Yang[2]

[1] *Professor, Dept. of Fundamental Engineering ,Institute of Industrial Science, The University of Tokyo, Tokyo, Japan*
[2] *Research Fellow, ESnS Structure Research Center, Kwangwoon University, Seoul, Korea*
Email: iisnak@iis.u-tokyo.ac.jp, wjyang@kw.ac.kr

ABSTRACT :

In general, hysteresis models that are applied to a numerical analysis part of substructure online tests do not refer directly to the experimental behavior of the members or subassemblage under loading tests. The objective of this study is to develop a new experimental technique for substructure online tests based on nonlinear hysteretic characteristics estimated with a neural network. A new learning algorithm for the network applicable to substructure online tests is proposed, focusing on input layer variables and their scaling method, and its validity is examined through several numerical and experimental investigations. The results show that the proposed testing scheme successfully reproduces the dynamic behavior of the model structure.

KEYWORDS : earthquake response, substructure online test, neural network, Ramberg-Osgood model

1. INTRODUCTION

To date, there have been carried out various experimental researches on seismic performance of structures. Among them, the substructure online test, also referred to as the hybrid pseudo-dynamic test, has been widely applied to simulate the earthquake response of structures. The substructure online test is an experimental technique to simulate the earthquake response of an entire structure combining a loading test of the structure's members or subassemblage and a numerical simulation of remaining part of the structure. Predetermined mathematical models are, however, generally used in the conventional substructure online tests to represent the hysteretic characteristics of numerical simulation part, and they would not take full advantage of the online testing technique that can directly incorporate the hysteretic characteristics under loading, unless the behavior of the simulation part is simple or fully understood prior to the online test. The testing technique, therefore, would be enhanced to be applied to more general structures if the online test can be performed without predetermined hysteretic models. To this end, the authors have tried to develop a method to estimate hysteretic characteristics of structural members and its application to the substructure online test, primarily focusing on the parallel formulation of a neural network through utilizing on-going loading test results.

In this paper, the formulation of a neural network which can be applied to the substructure online testing technique is discussed focusing on its structure, learning algorithm, etc. and their validity is verified through numerical and experimental investigations of model structures.

2. NEURAL NETWORK ALGORITHM

2.1. Multilayer Feed-Forward Neural Network

In this paper, a multilayer feed-forward neural network is used to estimate the hysteretic characteristics (i.e., the load-deflection relationship) of structural members or subassemblage. As shown in Figure 1, the network consists of three layers: an input layer, a hidden layer, and an output layer. As a learning algorithm of neural network, the back-propagation method is often applied in previous investigations by other researchers. Studies regarding the network training made by the authors et al., however, reveal that the whole learning method leads to greater success in saving computation time than the back-propagation method (Satoh et al. 2001). The whole learning method is therefore employed in this study as discussed in section 2.2.

Random numbers within the range of -0.5 to 0.5 are used as the initial values of the connection weight coefficient. The sigmoid function is used for the transfer function of input and hidden layers, while the linear function is used for the transfer function of the output layers. The transfer functions are shown in Figure 2.

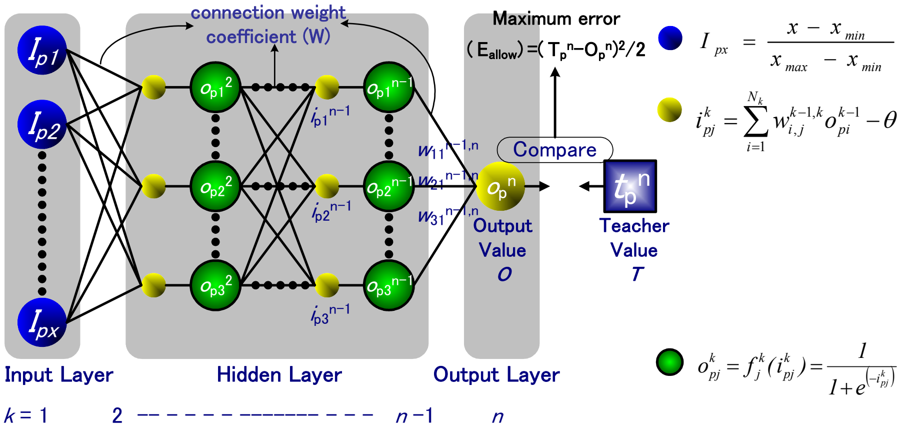

Figure 1 Multilayer feed-forward neural network

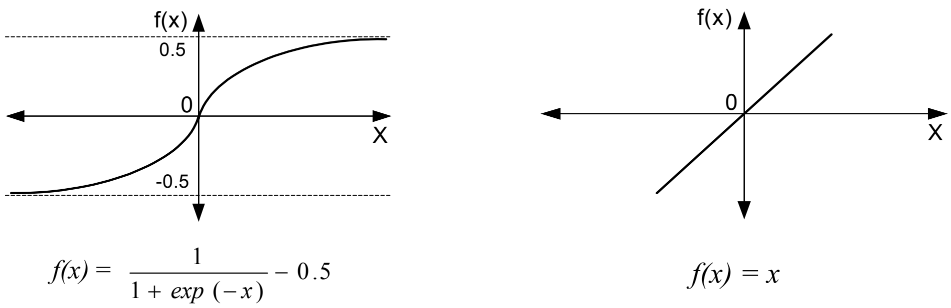

Figure 2 Transfer function (left: sigmoid function, right: linear function)

2.2. Whole Learning Algorithm

The learning of the feed-forward neural network is classified into a multi-objective optimization problem to minimize the error functions $f^{(n)}$ defined by Eq. (2.1) for all the training data sets, with respect to the weights associated with the connection between the units, where $O^{(n)}$ denotes the output from the network for the n-th set of the training data, $T^{(n)}$ the corresponding target value, and N the total number of training data sets.

$$f^{(n)} = \left| T^{(n)} - O^{(n)} \right| \quad (n=1, ..., N) \tag{2.1}$$

After the Taylor series expansion of $O^{(n)}$ with respect to ΔW_j, the error function $f^{(n)}$ is approximated by Eq. (2.2), where J denotes the total number of weights and W_j the value of the j-th weight.

$$f^{(n)} = \left| T^{(n)} - \left(O^{(n)} + \sum_{j=1}^{J} \frac{\partial O^{(n)}}{\partial W_j} \Delta W_j \right) \right| \quad (n=1, ..., N) \tag{2.2}$$

The error function by Eq. (2.2) can be rewritten with respect to all the training data sets, as shown in Eq. (2.3):

$$\{f\} = \{b\} - [B]\{\Delta W\} = \{0\} \qquad \{b\} = \left\{T^{(n)} - O^{(n)}\right\} \ , \ [B] = \left[\sum_{j=1}^{J} \frac{\partial O^{(n)}}{\partial W_j}\right] \tag{2.3}$$

where $[B]$ is the $N \times J$ rectangular matrix of coefficients, $\{b\}$ is the constant vector of N components, and $\{\Delta W\}$ is an unknown variable vector. The solution of the unknown variable vector $\{\Delta W\}$ is determined by using the Moore-Penrose generalized inverse, as shown in Eq. (2.4).

$$\{\Delta W\} = [B]^{-}\{b\} \qquad [B]^{-} \ : \text{Moore-Penrose generalized inverse} \tag{2.4}$$

2.3. Structure of Neural Network

The structure of the multilayer feed-forward neural network is shown in Table 1. In this study, two cases of input layers, Input Layer A and B, are investigated as shown in Table 1. The Input Layer A has five variables of (1) maximum displacement, (2) maximum restoring force, (3) displacement at latest turning point, (4) restoring force at latest turning point, and (5) current displacement. It should be noted that the variables (1) through (4) are determined over the range of loading steps 1 to i-1, while the variable (5) is corresponding to the current loading step i. The Input Layer B has two variables (1) maximum turning displacement and (2) maximum turning restoring force, and other three variables that are the same as (3) through (5) of Layer A.

Since there are no clear criteria to determine the appropriate number of nodes in the hidden layer, this study introduces the algorithm studied by Joghataie et al. (1995). The hidden layer starts with five nodes, which are the same number as the input layer, and their number automatically increases if necessary as learning is repeated, as will be described later in detail. The output value, i.e., the estimated results with the neural network, is the restoring force at the current displacement (input variable (5)) for both cases of Input Layers A and B.

2.4. Scaling of Input Layer Variables

All data to be learned are generally given prior to learning of the multilayer feed-forward neural network, and they are usually scaled with the known minimum and maximum values of each variable in the input layer (conventional method). Since the number of input data N to be learned herein, however, increases as the loading test progresses, the minimum and maximum values of the response can not be determined prior to the online test. In this study, two scaling methods are proposed and their applicability to online tests is investigated as well as the conventional method.

Investigated are the following three methods, i.e., (a) Conventional Method, (b) Method I, and (c) Method II. The minimum point ($X1'$, $P1'$) and the maximum point ($X2$, $P2$) on the load-deflection curve of a specimen are scaled in the following manner.

(a) Conventional Method: Each variable within ($X1'$, $P1'$) to ($X2$, $P2$) is scaled to the range of [-0.5, 0.5] depending on its minimum and maximum values as shown in Figure 3(a).
(b) Method I: Each variable is subdivided into a displacement group (variables (1), (3), and (5) in Table 1) and a restoring force group (variables (2) and (4) in Table 1). Symmetric ranges [-$X2$, $X2$] and [-$P2$, $P2$] are set for the displacement group and the restoring force group, respectively, and data in each group are then scaled to the range of [-0.5, 0.5] as shown in Figure 3(b).
(c) Method II: Each variable is subdivided into two groups and a symmetric range of displacement and restoring force is set [-0.5, 0.5] as is done in Method I. Note that a symmetric range of $[-\overline{P2}, \overline{P2}]$ instead of [-$P2$, $P2$] is used for the restoring force group, where $\overline{P2}$ is obtained using the initial stiffness and the displacement $X2$. As shown in Figure 3(c), data in each group are then scaled in the same manner of Method I described above.

The scaling above is made repeatedly when the maximum displacement is updated. Note that the methods I and II are introduced to re-scale data less frequently than the conventional method, and eventually are expected to result in shorter computation time. In particular, the method II is expected to have much shorter computation time due to significantly less frequent re-scaling of restoring force than other two methods.

Table 1 Structure of neural network

Input Layer	A	(1) Maximum displacement ($\lvert X_{i-1}\rvert_{max}$) (2) Maximum restoring force ($\lvert P_{i-1}\rvert_{max}$) (3) Displacement at latest turning point (X^t) (4) Restoring force at latest turning point (P^t) (5) Current displacement (X_i)
	B	(1) Maximum turning displacement ($\lvert X^t_{i-1}\rvert_{max}$) (2) Maximum turning restoring force ($\lvert P^t_{i-1}\rvert_{max}$) (3) Displacement at latest turning point (X^t) (4) Restoring force at latest turning point (P^t) (5) Current displacement (X_i)
Hidden Layer		One layer, starting with five units
Output Layer		Current restoring force

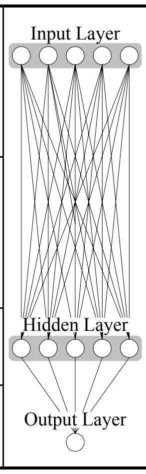

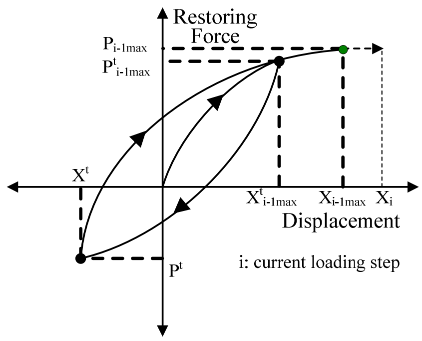

$\lvert X_{i-1}\rvert_{max}$: $\max(\lvert X_1\rvert, \ldots, \lvert X_{i-1}\rvert)$
$\lvert X^t_{i-1}\rvert_{max}$: $\max(\lvert X^t_1\rvert, \ldots, \lvert X^t_j\rvert)$, j: turning step
$\lvert P_{i-1}\rvert_{max}$: $\max(\lvert P_1\rvert, \ldots, \lvert P_{i-1}\rvert)$
$\lvert P^t_{i-1}\rvert_{max}$: $\max(\lvert P^t_1\rvert, \ldots, \lvert P^t_j\rvert)$, j: turning step

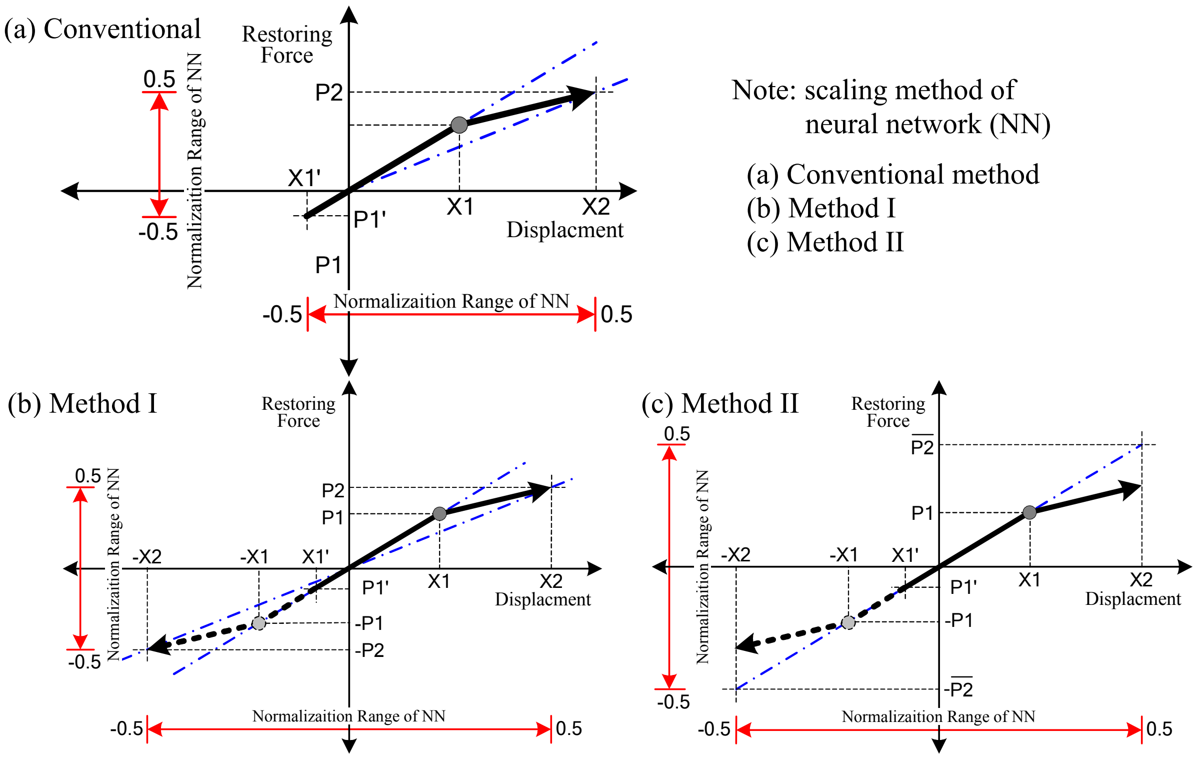

Figure 3 Data scaling for neural network

3. EARTHQUAKE RESPONSE ANALYSIS USING NEURAL NETWORK

3.1. Model Structure and Investigated Parameters

Numerical analyses are conducted to investigate the applicability of hysteresis modeling with a neural network that is constructed in parallel with a loading test. A prototype building shown in Figure 4(a) is studied in two cases. In the first case RR, the hysteretic rule of the first and second story is represented by the

Ramberg-Osgood (RO) model as shown in Figure 4(b). In the second case RN, as can be seen in Figure 4(c), the first story is represented by the RO model, and the second story is estimated by the neural network that learns the hysteretic characteristics of RO model in the first story while response computation.

In the RN analysis, two types of input layer A and B shown in Table 1, and three types of scaling methods shown in Figure 3, are considered as is shown in Table 2. The responses of RN model are then compared with those of RR model, which is deemed to have correct target responses. It should be noted that in the case of RN, the predicted restoring force at the current step i is fed back to define the input variables (2) and (4) shown in Table 1 in the subsequent computation step i+1.

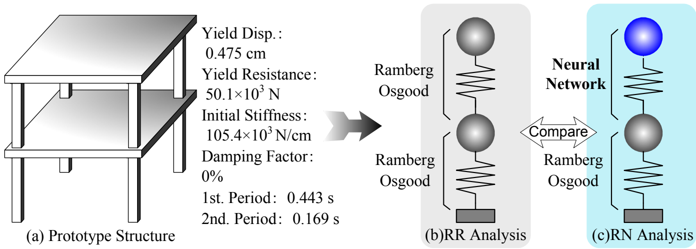

Figure 4 Modeling of structure

Table 2 Parameter of analyses

Case ID	Input Layer	Scaling
RR	**Target Response**	
RN	RN - A (Input layer A)	**Conventional Method (Fig 3(a))**
	RN - B (Input layer B)	
RNI	RN I-A (Input layer A)	**Scaling Method I (Fig 3(b))**
	RN I-B (Input layer B)	
RNII	RNII-A (Input layer A)	**Scaling Method II (Fig 3(c))**
	RNII-B (Input layer B)	

3.2. Numerical Integration and Input Earthquake Ground Motion

The Operator Splitting (OS) method is used for numerical integration of earthquake response analyses, and the time interval of the integration is set 0.01 second. Since the assessment of the earthquake response of a specific building is not the main purpose of this study, the damping effects are neglected in the analyses. For the input earthquake ground motions, used is an accelerogram for 20 seconds (a total of 2000 steps) including major motions of the NS component of the Chiba-ken Toho-oki earthquake recorded in 1987 at the Chiba Experiment Station of the Institute of Industrial Science, The University of Tokyo, Japan.

3.3. Convergence Conditions

In the nonlinear earthquake response analyses using the neural network hysteresis prediction technique, the prediction error is defined as $[T^{(n)} - O^{(n)}]^2 / 2$, and learning is made (maximum 100 times in one trial) under its allowable error of 10^{-4}. If the error is still larger than the allowable after 100 time learning, the connection weight coefficients (W) of the neural network are re-scaled with random numbers, and the learning procedure is re-performed. This procedure is repeated up to 20 trials. If the solution does not fall within the allowable error range after 20 trials, one more node is added in the hidden layer, and the same procedure (maximum 20 trials with 100 time learning in each trial) is again repeated. Since this study aims to apply a neural network to the substructure online test, it is favorable to avoid spending too much time for determining the network structure. Considering previous investigations by Yang et al. (2004), the number of nodes in the hidden layer is therefore limited to 12 (i.e., the number of nodes in the hidden layer may change within the range of 5 through 12), and the allowable error is increased from 10^{-4} to 10^{-3} if a satisfactory solution is not obtained until the number of nodes reaches 12. Furthermore, to reduce the learning time, learning is conducted in each response computation until the input acceleration attains the maximum value (PGA), and then learning after PGA is made only when the maximum response displacement is updated.

3.4. Analysis Results

The computed results are compared in Figures 5 and 6, and the time spent for the analyses is summarized in Table 3(CPU: Pentium IV, Xeon 1.4 GHz, 3650 Mflops), where most of the time is spent for network learning rather than response computation.

The case RN-A poorly reproduces the response and the computation is terminated at 900th step after 8 hours due to a large prediction error, while RN-B has fairly good agreement with RR results although the computation spends approximately 11 hours. RN II series shows excellent predictions and much shorter computation time than RN series and RN I series. As is found in Table 3, RN II-A shows 1/5 of RN I-A, and RN II-B shows 1/3 of RN I-B in computation time. These results suggest that the proposed scaling method II can be a promising candidate for its application to the substructure online test.

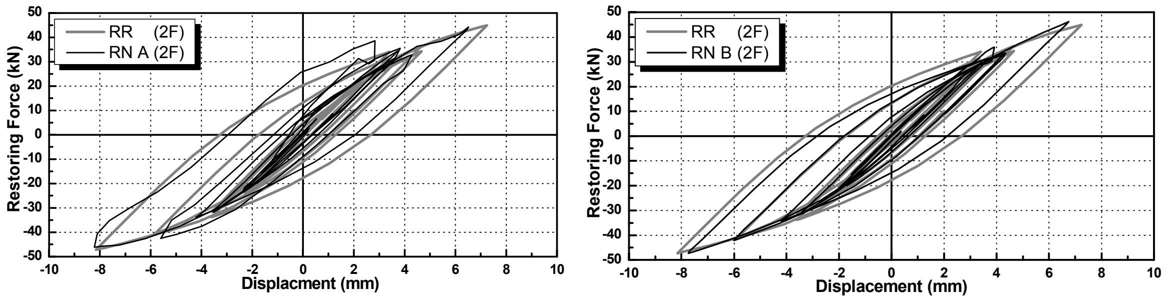

(a) 2nd story by RN-A (b) 2nd story by RN-B

Figure 5 Predicted earthquake response using conventional scaling method

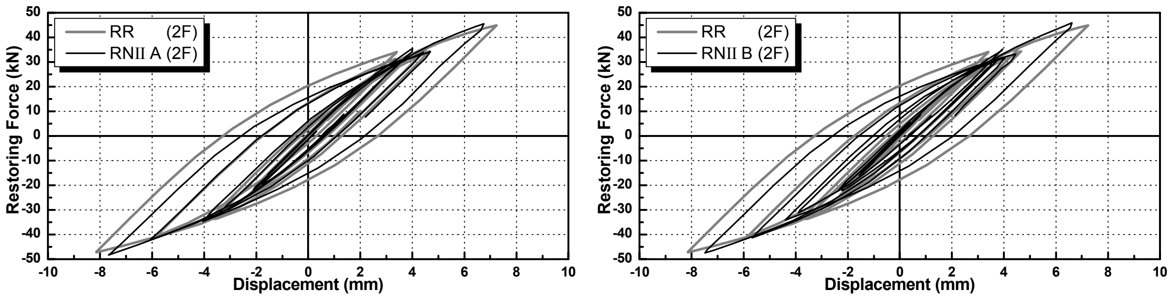

(a) 2nd story by RN II-A (b) 2nd story by RN II-B

Figure 6 Predicted earthquake response using scaling method II

Table 3 Computation time and number of nodes [CPU：Xeon 1.4 G, 3659 Mflops]

Case ID	Maximum Number of Hidden Layer Nodes		Computation Time (h:m:s)	Maximum Error*	Computation Terminated at
RN	RN - A (Input layer A)	12	Approx. 8 hrs	-	900th step
	RN - B (Input layer B)	12	Approx. 11 hrs	0.968	2000th step**
RN I	RN I-A (Input layer A)	12	04:09:00	0.968	2000th step**
	RN I-B (Input layer B)	12	03:03:00	0.968	2000th step**
RN II	RNII-A (Input layer A)	6	00:46:01	0.450	2000th step**
	RNII-B (Input layer B)	8	00:59:26	0.545	2000th step**

* Error at the step of computation terminated: $[T^{(n)}-O^{(n)}]^2/2$ ($\times 10^{-3}$) ** Response computations normally completed

4. SUBSTRUCTURE ONLINE TEST USING HYSTERETIC CHARACTERISTICS PREDICTED WITH NEURAL NETWORK

4.1. Specimens and Loading System

To verify the applicability and the effectiveness of the proposed scheme in the substructure online tests, four sets of specimens (OT, SOT1, SOT2, and NSOT) are made and tested under different loading control. Table 4 shows the test parameters. Each specimen is a simple two-degree-of-freedom system representing the prototype structure shown in Figure 7(a), and each test part is, as shown in the figure, replaced with 2 sets of identical H-shaped steel sections. The specimens are all taken from a single H-shaped steel member to minimize the test error associated with material uncertainties. As is employed in the numerical simulations, the NS component of the Chiba-ken Toho-oki earthquake, the OS method for numerical integrations, and an undamped system are applied in the response computation.

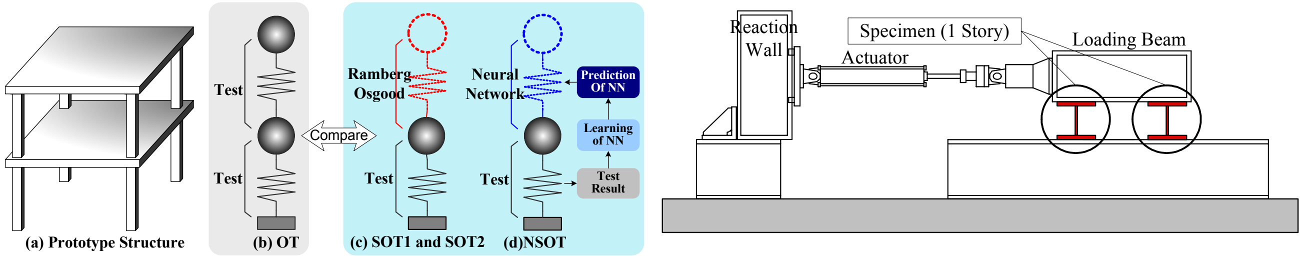

Figure 7 Test structures and loading system (Each story of OT is simultaneously loaded with two sets of the system.)

Table 4 Test parameters

Test	1st story	2nd story
OT	Test	Test
SOT 1	Test	RO model (The hysteretic loop shape parameters are determined from the geometric size and material properties ***prior to test***)
SOT 2	Test	RO model (The hysteretic loop shape parameters are determined ***after*** NSOT)
NSOT	Test	Predicted with neural network learning hysteresis of the first story ***during*** *test*

Specimen OT is tested to obtain a correct (or target) response to be compared with other test results. Each story is loaded using two sets of loading system shown in Figure 7. In specimen NSOT, a neural network that learns the load-deflection relationship in the first story is formed at every loading step, and the hysteretic loop in the second story is predicted using the network constructed in parallel with on-going substructure online test. In the test, a combination of the scaling method II and the input layer B is used in the network. Note that the predicted restoring force at the current step i is fed back to define the input variables (2) and (4) shown in Table 1 in the subsequent computation step i+1, as is done in previously discussed numerical simulations. Specimens SOT1 and SOT2 are made based on a conventional substructure online test scheme, where the first story is characterized from the loading test and the second story from a predetermined RO hysteretic rule. It should be noted that the shape parameters of the RO model are predetermined in SOT1 based only on the geometric size and material properties while they are determined in SOT2 considering the load-deflection curve obtained from the preceded NSOT results.

4.2. Test Results

Figure 8 shows the envelope curves of response in the first and second story of OT, SOT1, SOT2, and NSOT. As can be found in the figure, NSOT and SOT2 satisfactorily reproduce the response of OT while SOT1 significantly differs from OT. It should be pointed out that a poor reproduction of response in SOT1 can also be found in the first story because the prediction error made in the second story significantly affects the response in the loading story (i.e., first story). The precisely predicted hysteretic characteristics in the numerical simulation part, therefore, are most essential to successfully simulate the response of an entire structure.

Figure 9 shows the time history of response displacement, which again shows that NSOT as well as SOT2 can successfully reproduce the response of OT. Bearing in mind that the hysteretic shape parameters for RO model of SOT2 are determined from preceded test results while no shape parameters are needed prior to the loading test in NSOT, the proposed scheme has a major advantage over others because NSOT can simulate the correct response even if detailed structural information regarding the numerical simulation part of a structure is not available prior to the tests.

5. CONCLUSIONS

To establish the substructure online test technique using the hysteretic modeling with a neural network constructed in parallel with on-going loading test, the formulation of network is investigated focusing on its structure, learning algorithm etc. and their validity and applicability are examined through both numerical and

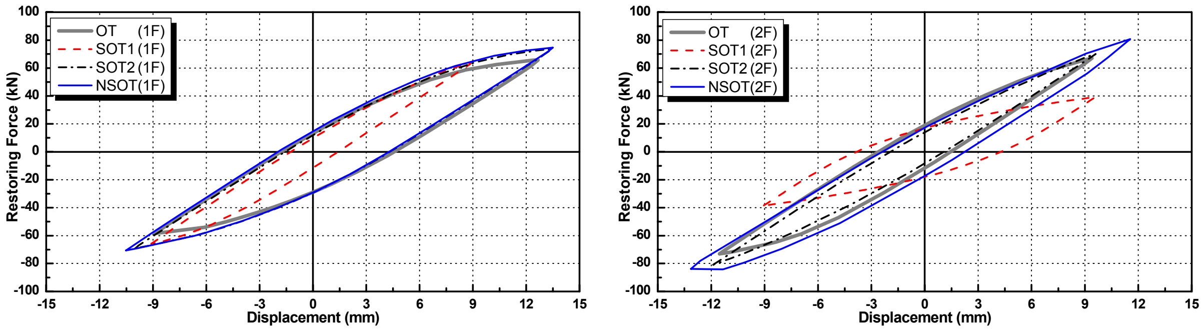

Figure 8 Envelope curves (left: 1st story, right: 2nd story)

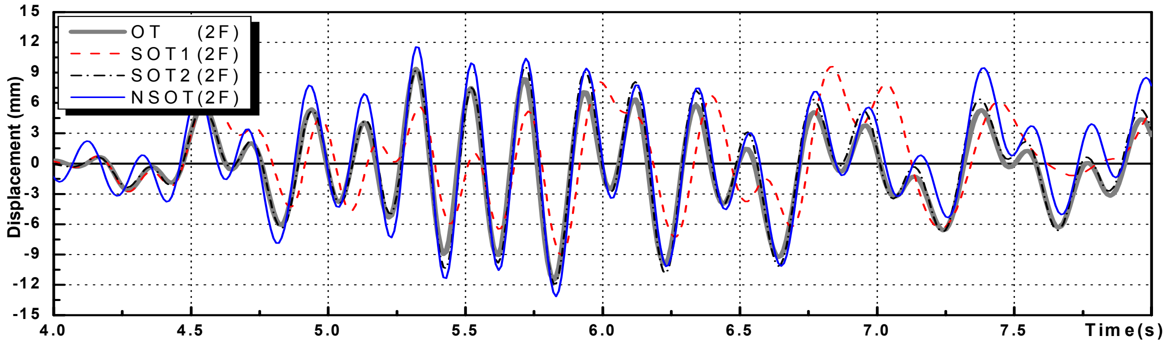

Figure 9 Comparison of response displacement in the 2nd story

experimental investigations. The major findings obtained in this study are summarized as follows:

1. The structure of the neural network employed in this study can be applied to predict the hysteretic characteristics of structural members. In particular, the scaling method II proposed herein can significantly reduce the learning time and improve the prediction performance even if the number of data to be learned increases as the loading test progresses.
2. The neural network with input layer B shows generally more successful and stable response prediction than that with input layer A, even when the extrapolation is needed in predicting the hysteretic rule.
3. The substructure online test using the scheme proposed in this study (NSOT) can satisfactorily reproduce the correct target response (OT). In particular, although the restoring forces predicted by the network are repeatedly used for subsequent input data, the network is robust enough and does not accumulate prediction errors to terminate the test. The proposed scheme therefore has a major advantage over others because NSOT can simulate the correct response even if detailed structural information regarding the numerical simulation part of a structure is not available prior to an online test.

ACKNOWLEDGEMENTS

This study was partially supported by the Grant-in-Aid for Scientific Research by the Ministry of Education of Japan (Principal Investigator: Yoshiaki Nakano, Grant No. 08875101).

REFERENCES

Satoh, K., Yoshikawa, N., Nakano, Y., and Yang, W. J. (2001). Whole Learning Algorithm of Neural Network for Modeling Nonlinear and Dynamic Behavior of RC Members. *Structural Engineering and Mechanics* **12:5,** 527-540.

Joghataie, A., Ghaboussi, J., and Wu, X. (1995). Learning and Architecture Determination through Automatic Node Generation. *Proceedings of International Conference on Artificial Neural Networks in Engineering*.

W. J. Yang, Y. Nakano, and Y. Sanada. (2004). Research on the Precision Improvement of the Substructure On-Line Test by Hysteresis Estimation Technique of Neural Network. *Journal of Structural Engineering, Architectural Institute of Japan* 2004; **50B**, 287-292.